



Investigation of Displacements in Tunnel-Constructed Liquefiable Soils with Numerical Analysis

*Makale Bilgisi / Article Info

Alındı/Received: 10.07.2023

Kabul/Accepted: 07.03.2024

Yayımlandı/Published: 29.04.2024

Tünel İnşa Edilmiş Sıvılaştırılabilir Zeminlerdeki Yer Değiştirmelerin Sayısal Analizlerle İncelenmesi

İsa VURAL , Dua KAYATÜRK* , Ayşe SAÇAR 

Department of Civil Engineering, Sakarya University of Applied Sciences, 54050, Sakarya, Turkey

© Afyon Kocatepe Üniversitesi

Abstract

The rise in industrialization and population has led to an increase in the economic significance of existing urban areas, and thus the utilization of underground space has become quite remarkable. It is an undeniable fact that in seismically active regions, the underground areas are also exposed to the risk of earthquakes. The devastating 1995 Kobe-Japan, 1999 Chi-Chi-Taiwan and 1999 Kocaeli-Turkey earthquakes are known to have caused major damage to existing underground structures. In this study, numerical models based on finite differences in FLAC 2D were established to evaluate the displacements of the ground around the tunnels located in liquefiable soils. In order to represent the liquefaction condition in the models, soils in the Adapazarı region, which have alluvial characteristics, were used. Soil deformations were examined in models with varying tunnel depths and diameters, for both liquefiable and non-liquefiable soils within the same layers. As a result of this study, it is stated that more stability losses are observed in analyzes where liquefaction can be defined - that is, changes in pore water pressures can be modeled - compared to analyzes without liquefaction. The layout of the ground layers is important for the positioning of the tunnel. The placement of the tunnel towards the solid layers caused the deformations to decrease.

Anahtar Kelimeler: Liquefiable soils; FLAC 2D; Tunnel; Adapazarı soils

Öz

Sanayileşme ve nüfustaki artış, mevcut kentsel alanların ekonomik öneminin artmasına yol açmış ve böylece yeraltı alanlarının kullanımı oldukça dikkat çekici hale gelmiştir. Sismik açıdan aktif bölgelerde yeraltı alanlarının da deprem riskine maruz kaldığı yadsınamaz bir gerçektir. Yıkıcı 1995 Kobe-Japonya, 1999 Chi-Chi-Tayvan ve 1999 Kocaeli-Türkiye depremlerinin mevcut yeraltı yapılarında büyük hasara neden olduğu bilinmektedir. Bu çalışmada, sıvılaştırılabilir zeminlerde bulunan tünellerin etrafındaki zeminin yer değiştirmelerini değerlendirmek için FLAC 2D'de sonlu farklara dayalı sayısal modeller kurulmuştur. Modellerde sıvılaşma durumunu temsil etmek için Adapazarı bölgesindeki alüvyon karakterli zeminler kullanılmıştır. Zemin deformasyonları, aynı katmanlardaki hem sıvılaştırılan hem de sıvılaşmayan zeminler için değişen tünel derinlikleri ve çaplarına sahip modellerde incelenmiştir. Bu çalışma sonucunda, sıvılaşmanın tanımlanabildiği, yani boşluk suyu basınçlarındaki değişimlerin modellenemediği analizlerde, sıvılaşma olmayan analizlere göre daha fazla stabilite kaybı gözlemlendiği belirtilmektedir. Zemin katmanlarının yerleşimi, tünelin konumlandırılması için önemlidir. Tünelin sağlam katmanlara doğru yerleşmesi deformasyonların azalmasına neden olmuştur.

Keywords: Sıvılaştırılabilir zeminler; FLAC 2D; Tünel; Adapazarı zeminleri

1. Introduction

The necessity for underground constructions is increased by rising urban land prices as well as rising domestic and municipal regulations. The tunnels are built in order to serve this need. There are numerous concerns associated with earthquakes for the tunnels in seismically active locations. As the tunnels serve as transportation, irrigation utilities, and storage areas, even minor damage can affect the serviceability of the tunnel (Wang and Zhang 2013). Seismic damage to underground structures is notably less severe in comparison to the harm suffered

by aboveground structures. The majority of damage to underground structures, such as tunnels, is primarily attributed to two factors: issues with the surrounding ground and the movement of the geological fault that the tunnel intersects (Wang et al. 2021). Despite the general safety advantage of underground structures compared to aboveground ones in seismic events, notable instances of seismic damage have been observed, such as the Daikai subway during the 1995 Kobe earthquake (Iida et al. 1996), a tunnel collapse during the 1999 Chi Chi earthquake due to fault crossing (Ueng et al. 2001), and

part of the Bolu tunnel collapsing during the 1999 Duzce earthquake (Hashash et al. 2001). These occurrences underscore the importance of considering seismic effects in tunnel design, emphasizing that such considerations should not be underestimated.

During seismic events, a noteworthy phenomenon frequently observed in alluvial soils is the occurrence of the soil liquefaction. In addition to structural damage caused by liquefaction, loss of life has also experienced in major earthquakes (Cetin et al. 2002). The liquefaction constitutes one of the most critical aspects of the design of structures, as it is one of the most important factors that cause stability loss in underground facilities as well as aboveground structures (Huang and Yu 2012). Due to underground structures pass through extensive areas, they are significantly affected by complex geological conditions. The liquefaction can also become an event that can seriously affect the seismic performance of the underground structure (Zhuang et al. 2015). Uplift of manholes, underground tanks and tunnel parts due to the floatation effect of liquefaction on underground structures has been observed in major earthquakes, such as 1964 Niigata, 2007 Noto Hanto, 2011 Christchurch (Mahmoud et al. 2020).

The considerations for conducting this study are as follows: the liquefaction induces substantial displacements in structures, and underground structures lack the capacity to accommodate such significant displacements. Therefore, the aim of this study is to evaluate the deformations that may occur in cases where liquefiable and non-liquefiable soils. In this numerical study, FLAC 2D software was used to model the pore water behavior at the time of the earthquake, which will enable liquefaction to occur.

2. Modelling

The advancement of technology has facilitated the utilization of numerous software tools, enabling enhanced analysis of underground and aboveground structures subjected to dynamic loads. This progress has resulted in improved modeling capabilities, reduced time requirements, and cost efficiencies. In this regard, modeling techniques such as the finite element method or the finite difference method can be utilized for accurate representation and analysis of these structures. FLAC (Fast Lagrangian Analysis of Continua) used in the numerical model studies in this study is a finite difference program that performs the Lagrangian analysis. The finite difference method is one of the oldest numerical

techniques used to solve differential equations by giving values such as initial conditions and boundary conditions. Firstly, FLAC establishes the equations of motion to generate new velocity and displacements from stresses and forces. And then calculates the deformation rates from the derivatives of the velocity and displacements obtained.

The linear elastic-plastic Mohr-Coulomb model was used for non-liquefiable soils. For liquefiable soils, Finn-Byrne liquefaction model was used to calculate the volumetric strains that occur during dynamic loading. With the Finn-Byrne model, the pore water pressures can be calculated from the volumetric strains, so that the excessive pore pressure and the liquefaction problems that will occur during earthquakes can be modeled (Byrne 1991). These models are documented in the Theory and Background Manual for FLAC (Itasca Consulting Group, Inc., 2000).

2.1 Soil Strata

In the present study, the region of Adapazarı was identified as the location for planned tunnel design. The decision to focus on the Adapazarı region stemmed from its positioning within a tectonically precarious area, coupled with the absence of existing tunnel structures in the vicinity. These factors served as primary motivations for the authors to undertake this research.

Geology of Adapazarı Region

Adapazarı is located in a 25x40 km² basin on the former lakebed. It contains quaternary alluvial soils carried by the Sakarya River. The bedrock can be reached at depths of about 200 m. The quaternary alluvial deposits contain lenticular or band-shaped low plasticity clay and silt series. The gravel, sand, clay, and silt are seen in some areas alone and different combinations in some areas (Kutunis et al. 2002).

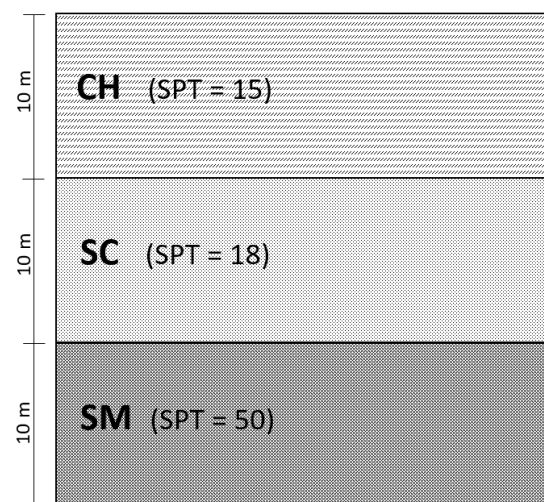


Figure 1. Schematic representation of soil layers

Table 1. Soil parameters

	Soil	Layer Height (m)	SPT	γ (kN/m ³)	ν	E (kN/m ²)	K (kN/m ²)	G (kN/m ²)	c (kN/m ²)	ϕ
Layer 1	CH	10	15	18	0.35	8100	9000	4200	40	1
Layer 2	SC	10	18	18	0.33	5600	5500	2600	1	30
Layer 3	SM	10	50	19	0.3	84000	70000	14800	1	39

CH: clay, SC: clayey sand, SM: silty sand (ASTM, 2006), γ : unit volume weight, ν : poisson ratio, E: Young's modulus, K: bulk modulus, G: shear modulus, c: cohesion, ϕ : angle of friction

Seismicity of Adapazarı Region

Adapazarı and its surroundings are under the influence of the North Anatolian Fault (NAF). The NAF is seismically one of the most important active faults in the world and is strike-slip fault forming. One of the reasons why the NAF is considered important is its similarity with the San Andreas fault in California, USA. These faults are similar in terms of neotectonic history, presence of creep, style of displacement, high seismicity, physiographic expression and problems of seismic-hazard evaluation (Allen 1982). Figure 1 depicts the soil model utilized in this article, which investigates the seismic behavior of tunnels constructed on alluvial and liquefiable soils. The objective is to ensure that the soil layers defined in the model accurately represent the Adapazarı region's soil composition. Detailed soil properties of the modeled soil can be found in Table 1. The SPT value is a soil resistance index measured by a standard sampler driven by a hammer falling a standardized distance. It assesses the soil's ability to withstand penetration. As the SPT value increases, it implies that the soil at that depth has greater shear strength, and in this study, the SPT value of the soil increases with depth.

2.2 Input Motion

The soil profile illustrated in Figure 1 were shaken by 1999 Kocaeli earthquake real strong motion data. The strong ground motion incorporated into the model was sourced

from the SKR station records available in the PEER database. The magnitude of the earthquake is $M_w=7.4$, the peak ground acceleration is $PGA=0.34$, the frequency range is 0.1-20. The acceleration-time graph of the earthquake is given in Figure 2.

2.3 Modeled Tunnels

The purpose of this study is to investigate the displacements that will occur in the tunnel and the soil under dynamic effects according to the depths, diameters and thicknesses of the tunnel. In order to study the displacements of the tunnel under dynamic effects, the models with different depths, diameters and thicknesses were created. With these models, the displacements of various tunnels subjected to dynamic effects were analyzed.

Vural (2012) conducted an analysis to determine the appropriate model size and observed that there were no changes in the accelerations after 30 meters horizontally and vertically. Based on this study, the model dimensions were determined as 30 m x 30 m, and the mesh intervals were defined as 50 cm. The objective of the analyses was to investigate the impacts of tunnel depth and diameter. To accomplish this, the models were created with tunnel depths of 10 m and 15 m, while the tunnel diameters varied between 4 m, 5 m, and 6 m. Additionally, the models were generated without tunnels in order to assess impacts based on depth only.

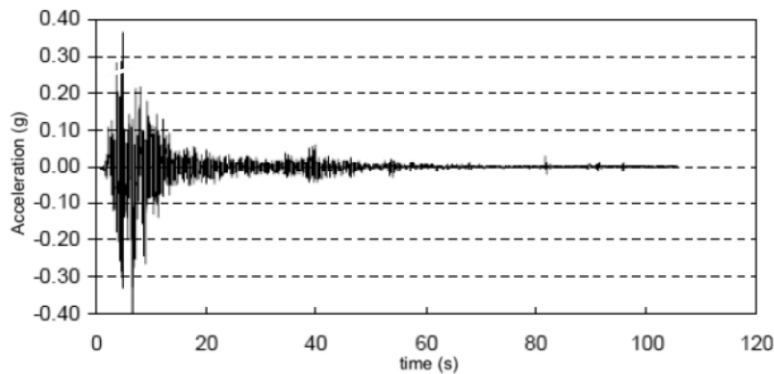


Figure 2. Recorded accelerogram of the Kocaeli Earthquake of 17 August 1999, SKR Station

Table 3. Tunnel material parameters

Shape	circle
Element	beam
Model	elastic
Mass density, ρ_s , kN/m^3	24
Young's modulus, E , GPa	38
Second moment of inertia, I , m^4	9.41
Cross-sectional area, A , m^2	0.548

The thickness effect is examined only in the non-liquefiable model, and thicknesses of 30 cm, 50 cm, and 100 cm were modeled. The dimensions of the modeled tunnels are given in Table 2.

By employing beam elements, which possess three degrees of freedom (x-translation, y-translation, and rotation) at each end node and can be interconnected with each other and/or the grid, circle-shaped tunnels were constructed. The structure is assumed to be elastic material. The material parameters defined for the 10 m depth, 4 m diameter, 30 cm thickness tunnel are given in Table 3.

The determination of boundary conditions holds significant importance in numerical model creation. Reflection of dynamic waves affects the accuracy of

analysis results. The FLAC 2D implements damping boundary conditions to prevent wave reflections at model boundaries and to allow smaller dimensions in dynamic analysis. In this research, the free-field boundary conditions of FLAC 2D were used as boundary conditions to ensure the continuity of the soil in the discretization of the infinite soil domain and to prevent wave reflections at the boundaries.

The tunnel cross-sectional shape is circular. The center of the 10 m deep tunnel is located at $x=15$ m, $y=20$ m, and the center of the 15 m deep tunnel is situated at $x=15$ m, $y=15$ m (The below point of the model is the $y=0$ point.) The mesh of the model set up for the tunnel with a depth of 10 m and the specific points where the displacements were examined in the study are shown in Figure 3a. Additionally, the depths, diameters and thicknesses of the modeled tunnels are given in Figure 3b, c, d respectively.

Liquefaction is a geotechnical phenomenon characterized by the loss of soil's load-bearing capacity and significant deformation due to excessive increases in pore water pressures under dynamic loading conditions. During the soil liquefaction, a significant decrease is observed in the shear strength and stiffness of the soils, which is caused by the increase in pore water pressure during the earthquake.

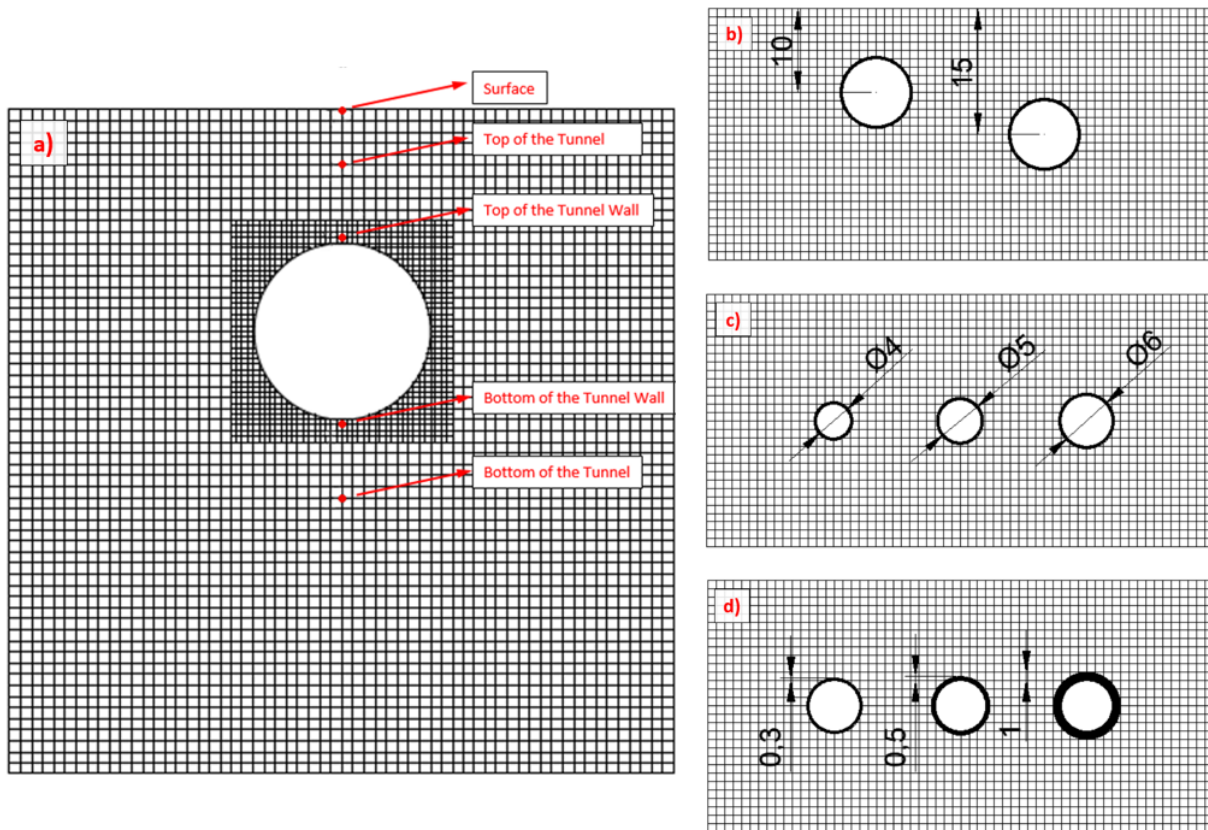


Figure 3. (a) The examined points of the model; (b) tunnel depths (m); (c) tunnel diameters (m); (d) tunnel thicknesses (cm)

The increase in the pore water pressure will trigger liquefaction; thus, the soil, which behaves like a liquid, will cause a loss of stability in the structures. In this study, two different constitutive models are used to examine the effect of liquefaction by numerical analysis; Mohr-Coulomb and Finn-Byrne.

Existing literature suggests that increasing the thickness of tunnel walls in liquefiable soils does not result in substantial changes in pore water pressure, thereby indicating negligible impact on liquefaction (Azadi and Hosseini 2010, Unutmaz 2014). Therefore, only the effects of varying the thickness of the tunnel walls in the dynamic models without liquefaction were examined.

3. Analysis Results

This study focuses on investigating the displacements that will arise from liquefaction induced by the dynamic effects of a tunnel on Adapazari soils. The Mohr-Coulomb constitutive model for non-liquefiable soils, the Finn-Byrne constitutive model has been used for the liquefiable soils. For the soil layers illustrated in Figure 1, the SC soil at depths of 10 m-20 m is identified as

liquefiable soil, and thus, the Finn-Byrne model has been employed to characterize this specific layer. The horizontal and vertical displacements of five distinct points within the soil are provided in this section for the models.

Figure 4 presents a comparative analysis of horizontal displacements for three scenarios: without a tunnel, with a tunnel at a depth of 10 m, and with a tunnel at a depth of 15 m. The horizontal displacements are examined and compared using both the Mohr-Coulomb and Finn-Byrne models. Similarly, Figure 5 provides a comparison of vertical displacements for the same three scenarios as Figure 4, also utilizing the Mohr-Coulomb and Finn-Byrne models. Moving on to Figure 6, it focuses on horizontal displacements and compares them for three different tunnel diameters: 4 m, 5 m, and 6 m. The displacements are assessed using both the Mohr-Coulomb and Finn-Byrne models. Lastly, Figure 7 parallels the examinations conducted in Figure 6, but specifically for vertical displacements, comparing the same three tunnel diameters using the Mohr-Coulomb and Finn-Byrne models.

Horizontal Displacement for Mohr-Coulomb Model

Horizontal Displacement for Finn-Byrne Model

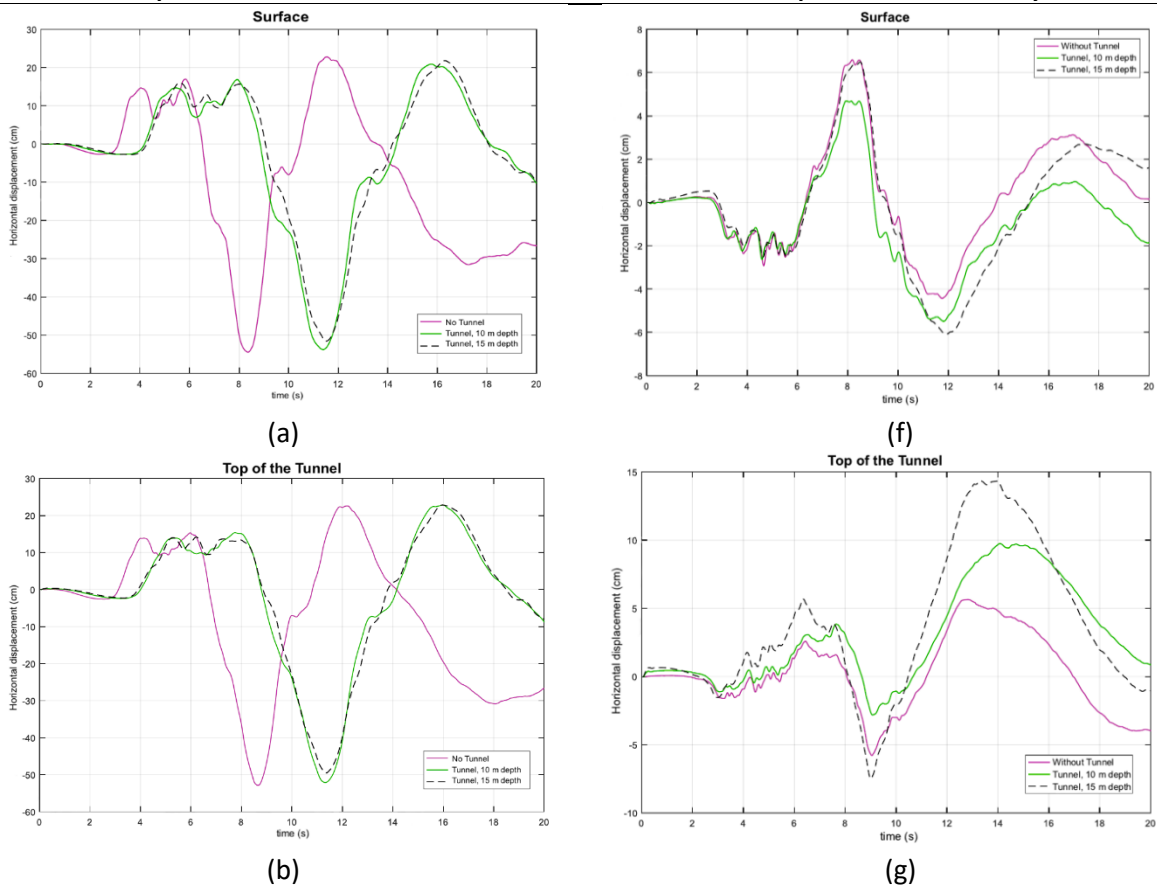


Figure 4. Horizontal displacements by depth; (a), (b), (c), (d), (e) Mohr-Coulomb model; (f), (g), (h), (i), (j) Finn-Byrne model; (a), (f) at surface; (b), (g) at top of the tunnel; (c), (h) at top of the tunnel wall; (d), (i) at bottom of the tunnel wall; (e), (j) at bottom of the tunnel

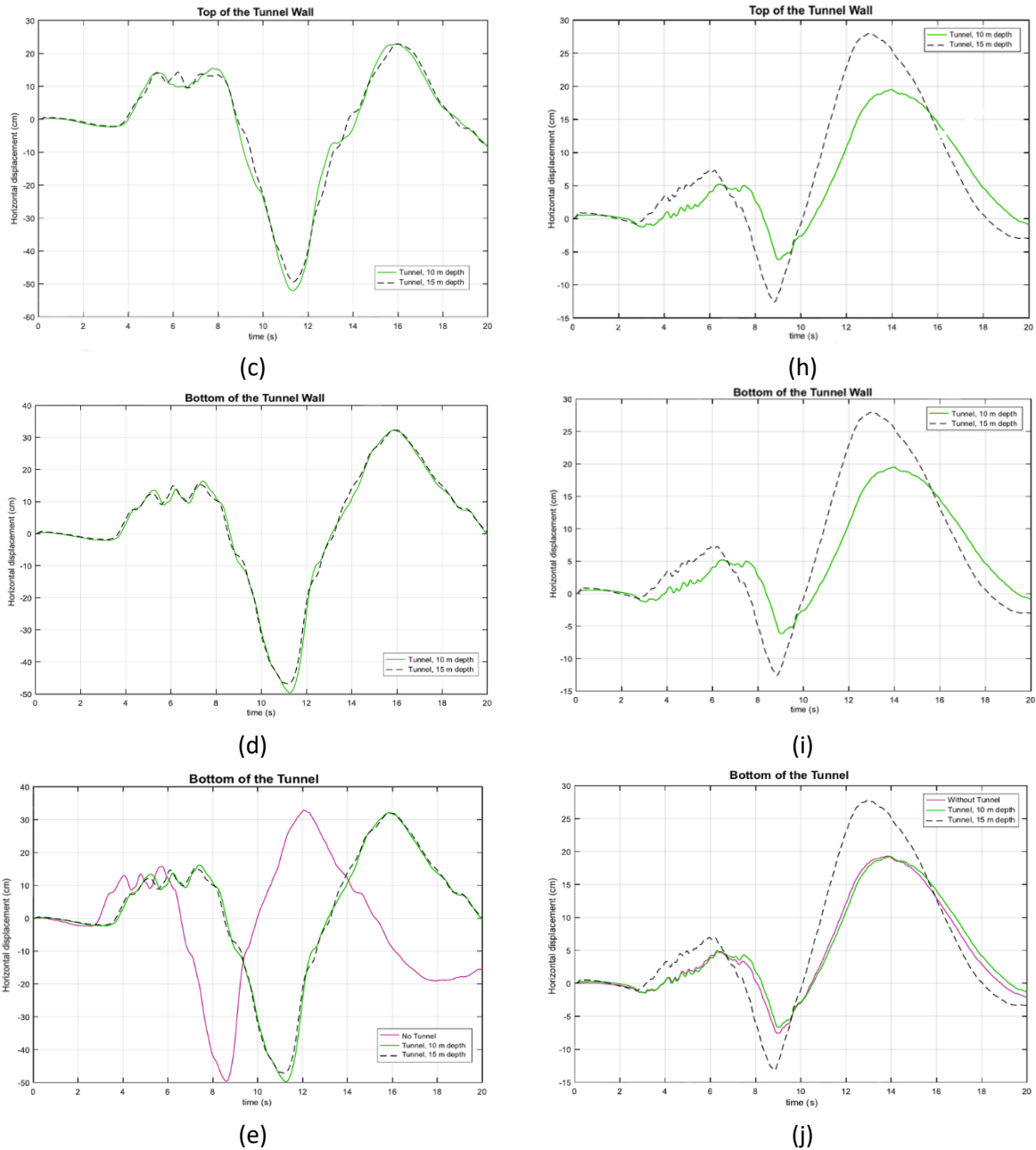


Figure 4. (Continued) Horizontal displacements by depth; (a), (b), (c), (d), (e) Mohr-Coulomb model; (f), (g), (h), (i), (j) Finn-Byrne model; (a), (f) at surface; (b), (g) at top of the tunnel; (c), (h) at top of the tunnel wall; (d), (i) at bottom of the tunnel wall; (e), (j) at bottom of the tunnel

As demonstrated in the acceleration time graph of the Kocaeli earthquake given in Figure 2, the time interval in which the energy of the earthquake and therefore the displacements due to the earthquake is the highest in the first 20 seconds. The main discharge time of the energy occurred in the first 20 seconds. In dynamic analysis, especially the first 20 seconds of earthquake will create peak values in terms of displacements. The decrease in the energy of the earthquake after 20 seconds will mean that the displacements due to the earthquake will not reach peak values after 20 seconds. The ultimate displacements (displacements at 20 sec) are also given in

Table 4, as it gives the chance to interpret the change in the same time period in different constitutive models. In Figures 4 and 5, the graphs of displacements of models with a diameter of 5 m without a tunnel, with a center at 10 m and with a tunnel at 15 m are given. In Figure 4, it is observed that the horizontal displacements of the tunnels at different depths are approximately 3 times higher in non-liquefiable soils than in liquefiable soils, the bottom of the tunnel wall point for the tunnel located at the central 10 m remained within the liquefiable soil layer in both models (Figure 4d, 4i). It can be said that different behaviors are observed in this study using two different

constitutive models. In the Mohr-Coulomb model, it can be concluded that failure occurs due to the load exceeding, and therefore the deformations are higher. In addition, in the Mohr-Coulomb model, it is seen that the displacements at the five points examined on the soil are very close to each other, which shows that the same soil behavior is observed at every point in the Mohr-Coulomb constitutive model. According to the findings in the Finn-Byrne model, it is evident that the horizontal displacements at the tunnel wall points located near the underground structure are greater compared to the upper points of the tunnel. This observation suggests that the structure within the soil is more susceptible to dynamic movements, resulting in increased ground motion around the structure. Based on Figure 4, a

comparison between the Finn-Byrne and Mohr-Coulomb models reveals that the soil experiences less movement with the tunnel in the former model. This suggests that the tunnel tends to maintain its horizontal position due to the presence of liquefaction. Furthermore, in the absence of a tunnel, it can be observed that the bottom point of the tunnel, one of the points under investigation, remains within the liquefiable soil layer at a depth of 10 m-20 m. In contrast, the surface and top points of the tunnel remain in the soil layer where liquefaction is not anticipated at a depth of 0 m-10 m. Significantly, in the liquefiable layer, horizontal displacements reach twice the magnitudes compared to the upper layer, indicating the higher levels of movement experienced in the layer prone to liquefaction.

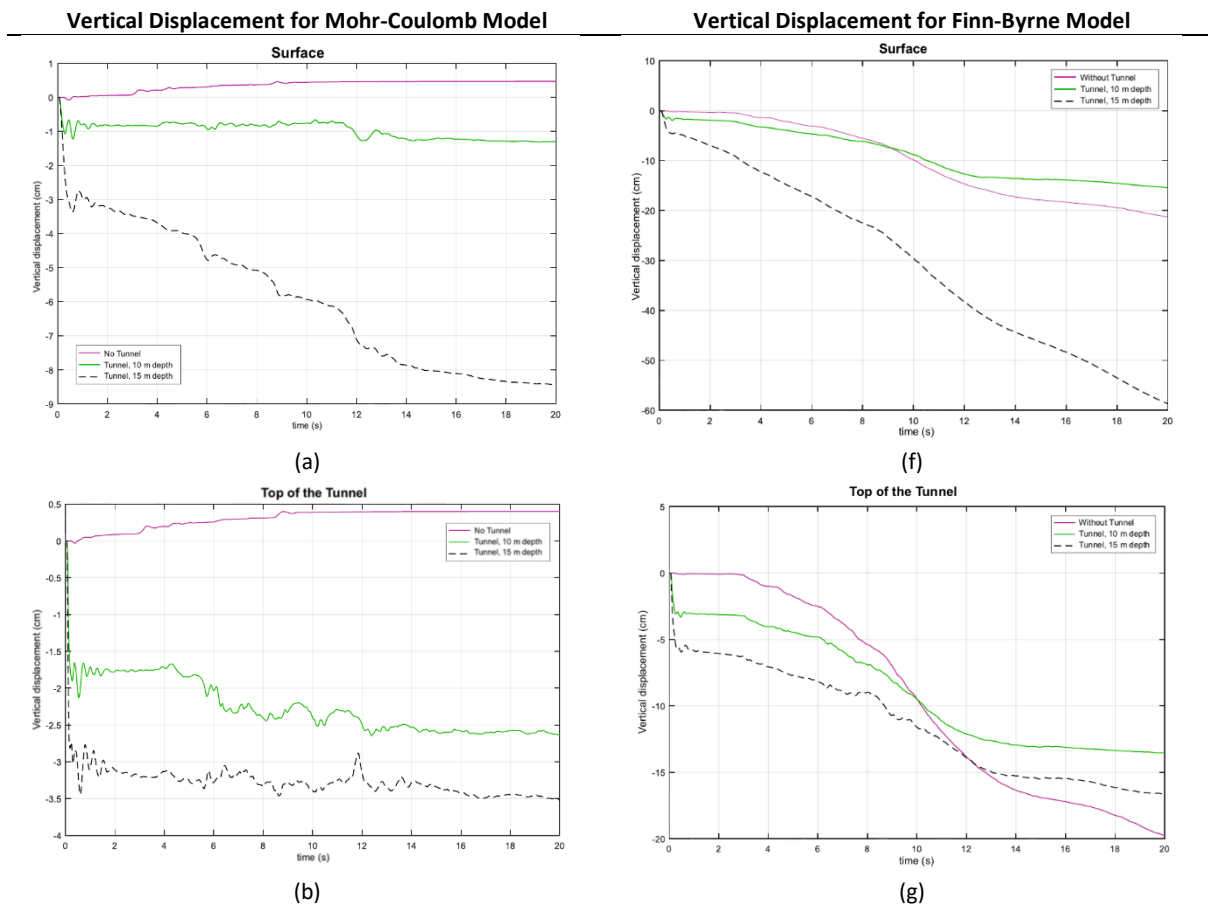


Figure 5. Vertical displacements by depth; (a), (b), (c), (d), (e) Mohr-Coulomb model; (f), (g), (h), (i), (j) Finn-Byrne model; (a), (f) at surface; (b), (g) at top of the tunnel; (c), (h) at top of the tunnel wall; (d), (i) at bottom of the tunnel wall; (e), (j) at bottom of the tunnel

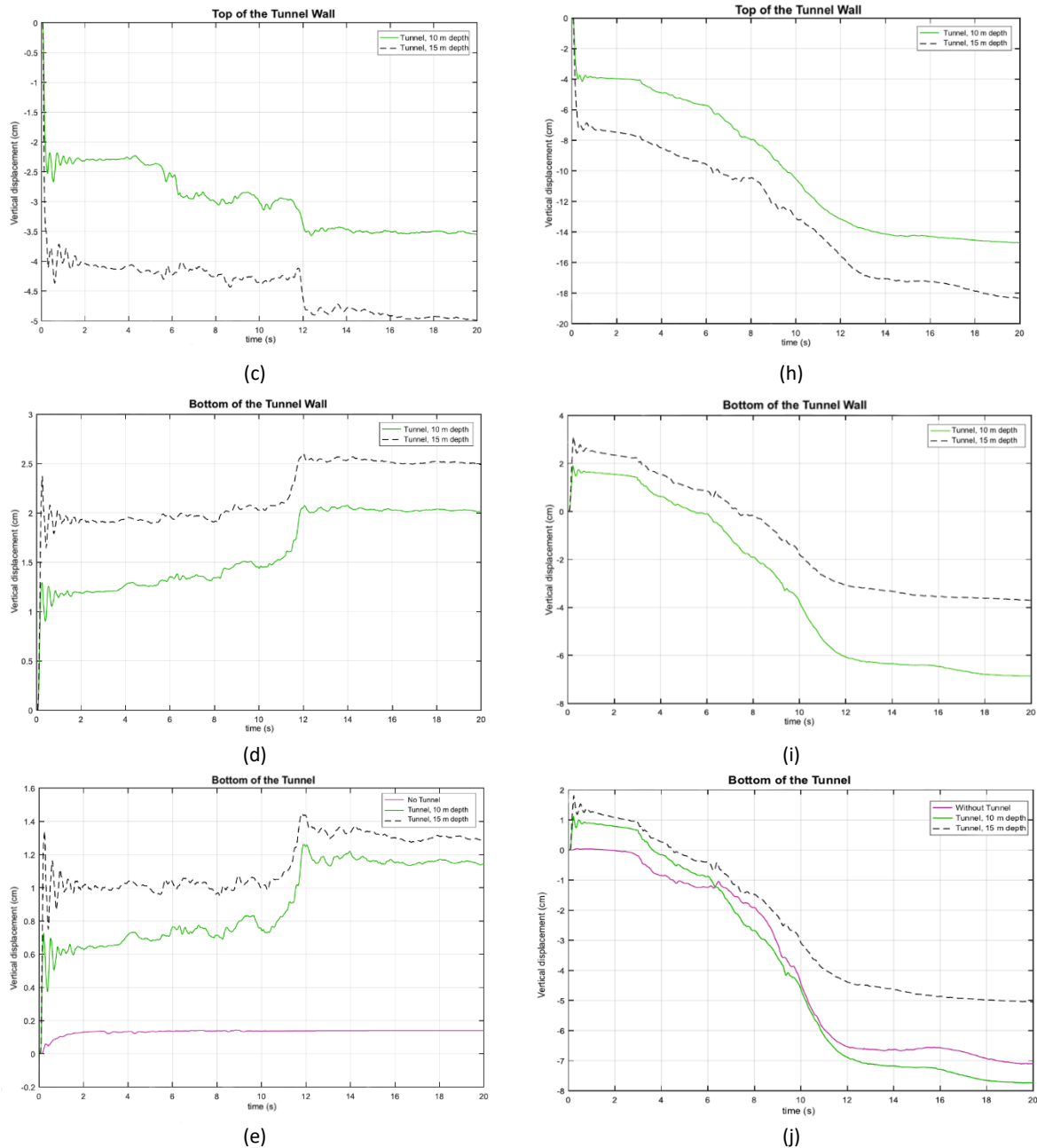


Figure 5. (Continued) Vertical displacements by depth; (a), (b), (c), (d), (e) Mohr-Coulomb model; (f), (g), (h), (i), (j) Finn-Byrne model; (a), (f) at surface; (b), (g) at top of the tunnel; (c), (h) at top of the tunnel wall; (d), (i) at bottom of the tunnel wall; (e), (j) at bottom of the tunnel

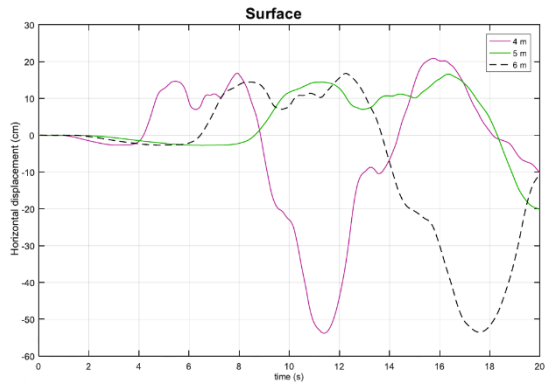
In Figure 5, the vertical displacements of tunnels at different depths are examined. Tunneling to deeper points in the Mohr-Coulomb model increased the displacements at the points above the tunnel (Figure 5a, b, c), in addition, it is seen that swelling occurs at the points under the tunnel. (Figure 5d, e).

Since the diameters of the tunnels at different depths are taken as 5 m in the Finn-Byrne model, the positive effect of the lowest soil layer, which is the firmer layer, on the horizontal deformations is seen (Figure 5i, 5j). Since the tunnel with its center located at 15 m will settle on more

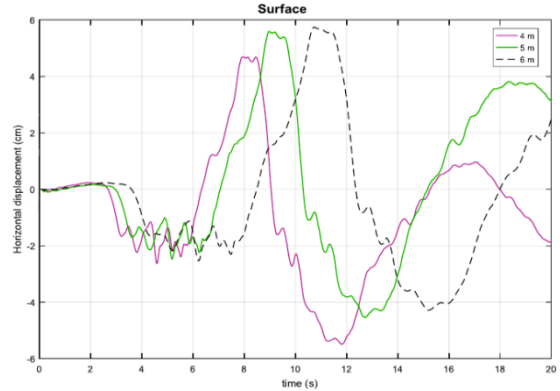
solid ground, the deformation center at the bottom of the tunnel has been less than the tunnel located at 10 m. When the Finn-Byrne model is compared with the Mohr-Coulomb model, it is seen that the vertical displacements increase approximately 5 times due to the liquefaction effect (Figure 5). Due to liquefaction, the vertical deformation center of the tunnel is located at 15 m, and the vertical deformation on the surface is higher than the other models (Figure 5a, 5f). The lower positioning of the tunnel has made it vulnerable to deformations that will occur as a result of dynamic effects, as it causes more soft soils on top.

Horizontal Displacement for Mohr-Coulomb Model

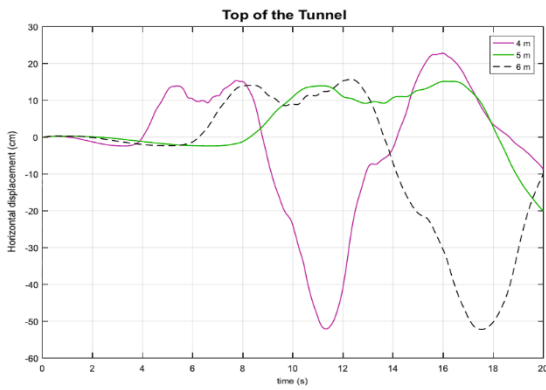
Horizontal Displacement for Finn-Byrne Model



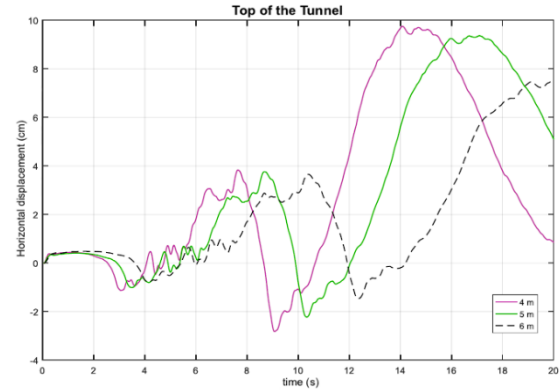
(a)



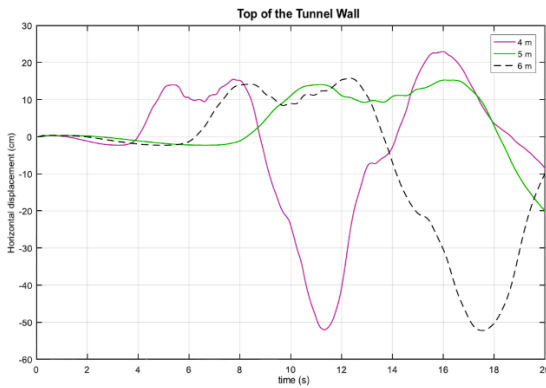
(f)



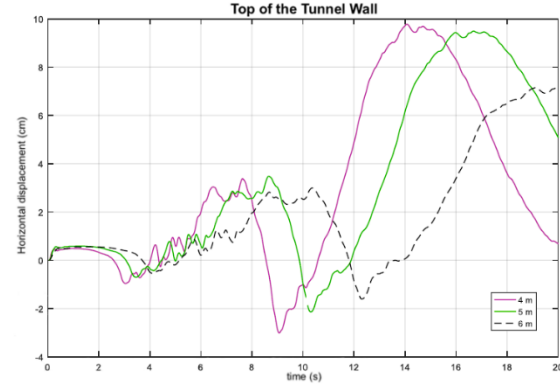
(b)



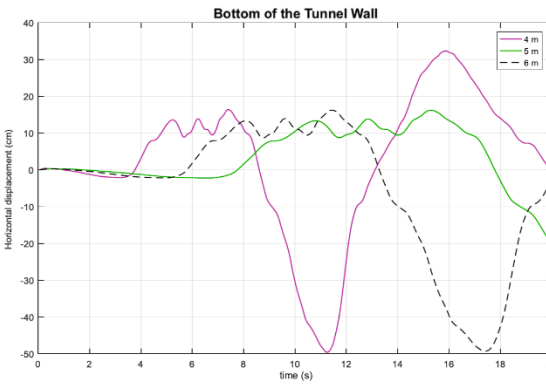
(g)



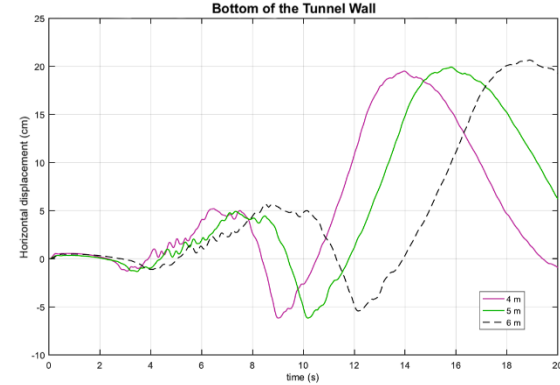
(c)



(h)



(d)



(i)

Figure 6. Horizontal displacements by diameter; (a), (b), (c), (d), (e) Mohr-Coulomb model; (f), (g), (h), (i), (j) Finn-Byrne model; (a), (f) at surface; (b), (g) at top of the tunnel; (c), (h) at top of the tunnel wall; (d), (i) at bottom of the tunnel wall; (e), (j) at bottom of the tunnel

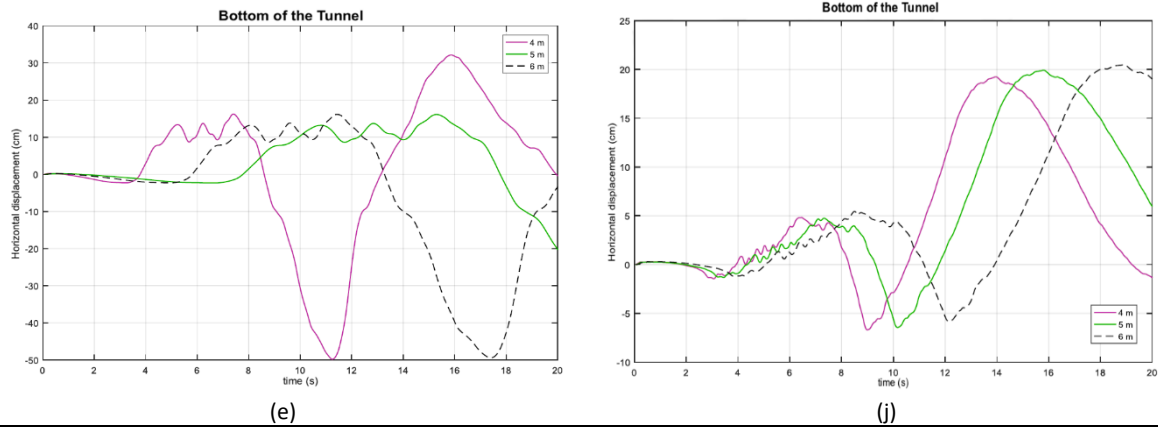


Figure 6. (Continued) Horizontal displacements by diameter; (a), (b), (c), (d), (e) Mohr-Coulomb model; (f), (g), (h), (i), (j) Finn-Byrne model; (a), (f) at surface; (b), (g) at top of the tunnel; (c), (h) at top of the tunnel wall; (d), (i) at bottom of the tunnel wall; (e), (j) at bottom of the tunnel

Figures 6 and 7 represent the displacement graphs of tunnels with varying diameters centered at 10 m. The diameters of these tunnels range from 4 m to 6 m. In Figure 7, the vertical displacements of tunnels with different diameters are investigated. According to the Finn-Byrne model, increasing the diameter of the tunnels leads to a reduction in vertical displacements at the points below the tunnel (as illustrated in Figures 7i and 7j).

Increasing the diameter of the tunnel means getting closer to the SM, which is the hardest layer in the models. It is worth noting that the vertical displacements in the Finn-Byrne model are approximately six times greater than those in the Mohr-Coulomb model. Additionally, horizontal displacements in liquefiable conditions result in higher displacements below the tunnel and under the tunnel wall compared to the areas above the tunnel.

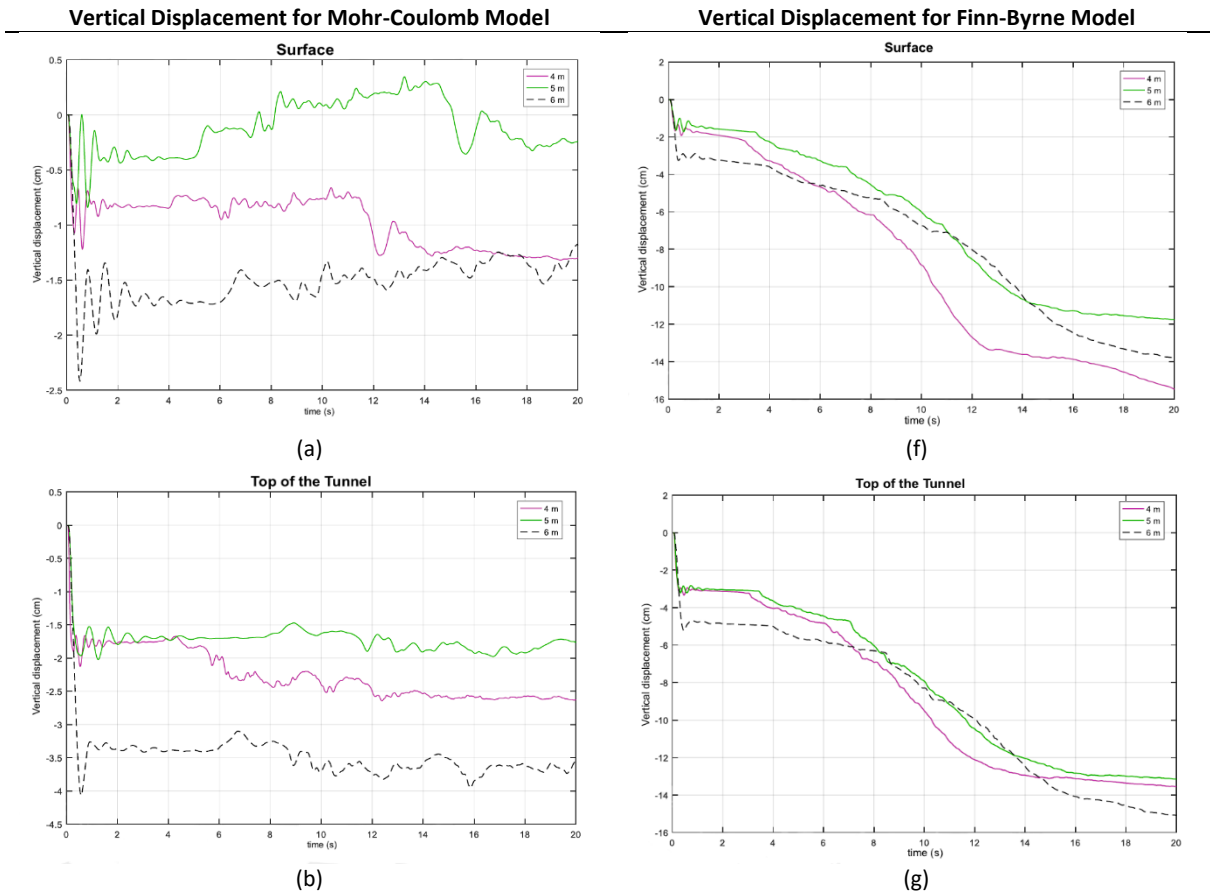


Figure 7. Vertical displacements by diameter; (a), (b), (c), (d), (e) Mohr-Coulomb model; (f), (g), (h), (i), (j) Finn-Byrne model; (a), (f) at surface; (b), (g) at top of the tunnel; (c), (h) at top of the tunnel wall; (d), (i) at bottom of the tunnel wall; (e), (j) at bottom of the tunnel

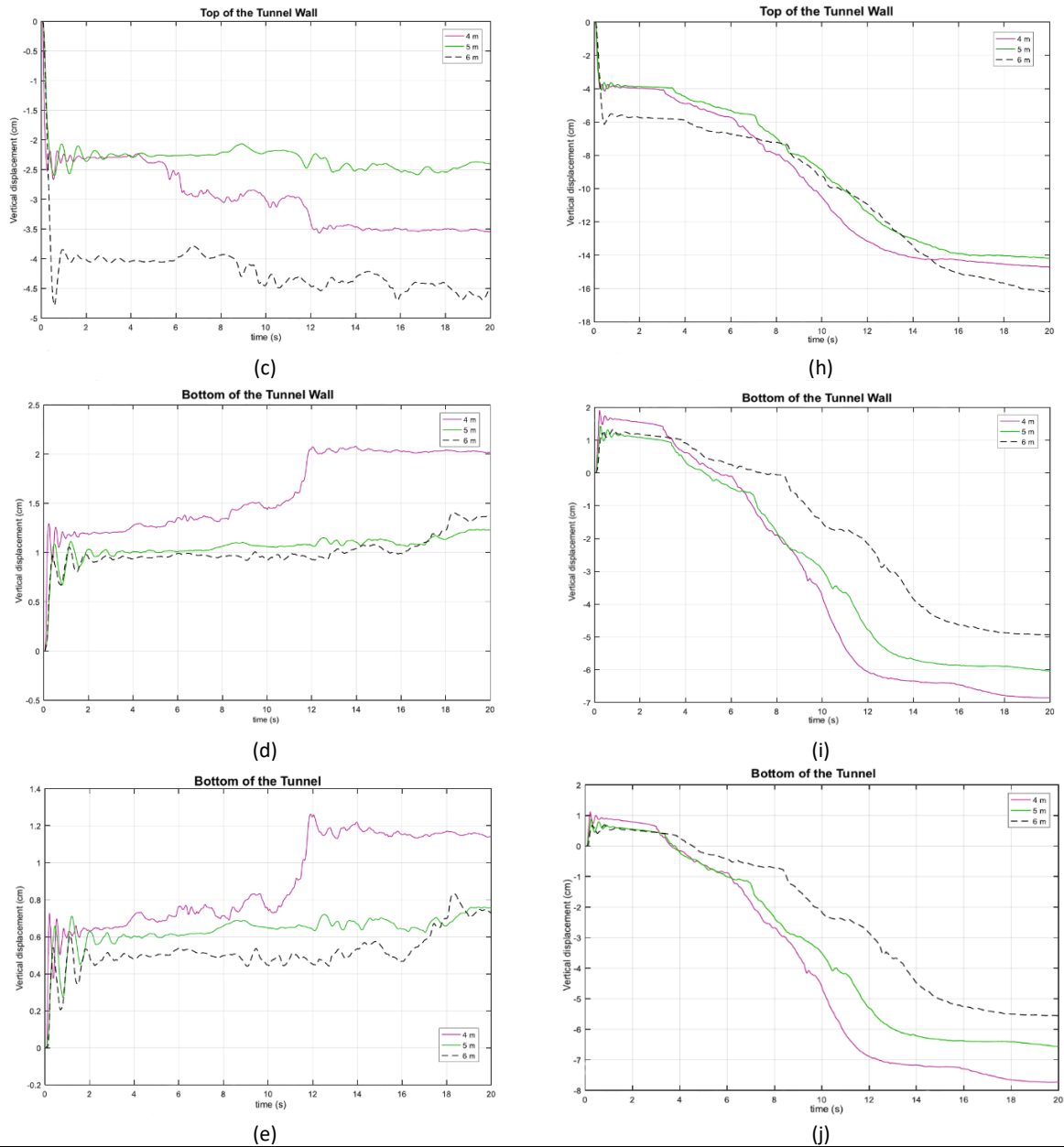


Figure 7. (Continued) Vertical displacements by diameter; (a), (b), (c), (d), (e) Mohr-Coulomb model; (f), (g), (h), (i), (j) Finn-Byrne model; (a), (f) at surface; (b), (g) at top of the tunnel; (c), (h) at top of the tunnel wall; (d), (i) at bottom of the tunnel wall; (e), (j) at bottom of the tunnel

The data from Figures 4, 5, 6 and 7 are summarized in Table 4. While the peak displacement defines the maximum and minimum values recorded during the 20 second earthquake, the displacements at the end of 20 seconds are given as ultimate displacements.

It has been mentioned in the studies of Azadi and Hosseini (2010), Unutmaz (2014) that different thicknesses of the tunnel wall do not have an effect on displacements in liquefiable soils. In this study, the effect of thickness on non-liquefiable soils is investigated. The obtained displacements data are given in Table 4. The tunnel wall thicknesses of 30 cm, 50 cm and 100 cm are determined in the models created. According to the analysis, it is seen that different tunnel wall thicknesses have no effect on displacements in non-liquefiable soils.

4. Conclusions

The rise in industrialization and population growth has amplified the economic significance of urban areas, consequently augmenting both domestic and municipal demands. The escalating challenges associated with constructing aboveground structures have propelled the prominence and necessity of underground structures. The tunnels are regarded as a viable solution to meet the growing needs of individuals and urban areas. As underground tunnels, which form the backbone of vital infrastructure systems, are susceptible to dynamic forces, their design necessitates adherence to specific conditions.

Table 4. The numerical analysis results

Mohr-Coulomb Model;

By Depth;	Mohr-Coulomb Model;																		
	Surface			Top of the Tunnel			Bottom of the Tunnel			Top of the Tunnel Wall			Bottom of the Tunnel Wall						
	No Tunnel	With Tunnel	10 m	4 m	5 m	6 m	No Tunnel	With Tunnel	10 m	15 m	With Tunnel	10 m	15 m	With Tunnel	10 m	15 m	With Tunnel	10 m	15 m
Peak Horizontal Disp. (cm)	+23, -55	+21, -55	+22, -52	+23, -53	+23, -53	+23, -50	+33, -50	+33, -50	+32, -50	+32, -47	+23, -52	+23, -50	+32, -46	+32, -50	+32, -46	+32, -50	+32, -46	+32, -50	+32, -46
Peak Vertical Disp. (cm)	+0.5	-1.3	-8.5	+0.4	-2.6	-8	-3.5	+0.15	+1.27	+1.45	-3.5	-5	+2.5	0	0	0	0	0	0
Ultimate Horizontal Disp. (cm)	-25	-10	-10	-27	-8	-8	-15	0	0	0	-8	-8	0	-8	-8	-8	-8	-8	-8
Ultimate Vertical Disp. (cm)	+0.5	-1.3	-8.5	+0.4	-2.6	-3.5	+0.15	+1.15	+1.3	+1.3	-3.5	-5	+2.5	+2	+2	+2	+2	+2	+2.5
By Diameter;																			
	Surface			Top of the Tunnel			Bottom of the Tunnel			Top of the Tunnel Wall			Bottom of the Tunnel Wall						
	4 m	5 m	6 m	4 m	5 m	6 m	4 m	5 m	6 m	4 m	5 m	6 m	4 m	5 m	6 m	4 m	5 m	6 m	
Peak Horizontal Disp. (cm)	+20, -54	+15, -20	+17, -53	+23, -52	+15, -20	+16, -52	+32, -50	+16, -20	+16, -50	+23, -52	+15, -20	+16, -52	+32, -50	+16, -20	+16, -52	+32, -50	+16, -20	+16, -52	+32, -50
Peak Vertical Disp. (cm)	-1.3	+0.3, -0.8	-2.4	-2.6	-2	-4	+1.28	+0.74	+0.84	-3.5	-2.6	-4.7	+2	+1.25	+1.4	+2	+1.25	+1.4	+1.4
Ultimate Horizontal Disp. (cm)	-10	-20	-10	-8	-20	-10	0	-20	-4	-8	-20	-10	0	-20	-4	-8	-20	-10	-4
Ultimate Vertical Disp. (cm)	-1.3	-0.25	-1.2	-2.6	-1.75	-3.5	+1.17	+0.74	+0.72	-3.5	-2.4	-4.5	+2	+1.25	+1.4	+2	+1.25	+1.4	+1.4
By Thickness;																			
	Surface			Top of the Tunnel			Bottom of the Tunnel			Top of the Tunnel Wall			Bottom of the Tunnel Wall						
	30 cm	50 cm	100 cm	30 cm	50 cm	100 cm	30 cm	50 cm	100 cm	30 cm	50 cm	100 cm	30 cm	50 cm	100 cm	30 cm	50 cm	100 cm	
Peak Horizontal Disp. (cm)	+20, -53	+20, -52	+20, -51	+22, -52	+22, -51	+22, -50	+32, -50	+32, -50	+32, -50	+23, -52	+23, -51	+23, -50	+32, -50	+32, -49	+30, -48	+32, -50	+32, -49	+30, -48	
Peak Vertical Disp. (cm)	-1.35	-1.3	-1.25	-2.6	-2.6	-2.6	+1.27	+1.27	+1.27	-3.5	-3.5	-3.5	-3.5	+2	+2	+2	+2	+2	
Ultimate Horizontal Disp. (cm)	-10	+2	+20	-10	+4	+22	0	+15	+30	-8	+5	+22	0	+15	+30	0	+15	+30	
Ultimate Vertical Disp. (cm)	-1.35	-1.3	-1.25	-2.6	-2.6	-2.6	+1.18	+1.18	+1.18	-3.5	-3.5	-3.5	+2	+2	+2	+2	+2	+2	

Finn-Byrne Model;

By Depth;	Finn-Byrne Model;																		
	Surface			Top of the Tunnel			Bottom of the Tunnel			Top of the Tunnel Wall			Bottom of the Tunnel Wall						
	No Tunnel	With Tunnel	10 m	4 m	5 m	6 m	No Tunnel	With Tunnel	10 m	15 m	With Tunnel	10 m	15 m	With Tunnel	10 m	15 m	With Tunnel	10 m	15 m
Peak Horizontal Disp. (cm)	+6.5, -4.3	+4.8, -5	+6.5, -6	+6, -6	+9, -2.5	+14, -7.5	+19, -7.5	+19, -7.5	+19, -7	+26, -13	+19, -6	+27, -13	+19, -6	+19, -6	+27, -13	+19, -6	+19, -6	+27, -13	
Peak Vertical Disp. (cm)	-22	-15	-58	-20	-14	-16	-7	-7.7	-7.7	-5	-15	-18.5	-7	-7	-3.7	-7	-7	-3.7	
Ultimate Horizontal Disp. (cm)	0	-2	+1.8	-4	+1	-1	-2	-1	-4	-4	-1	-3	-1	-1	-3	-1	-1	-3	
Ultimate Vertical Disp. (cm)	-22	-15	-58	-20	-14	-16	-7	-7.7	-7.7	-5	-15	-18.5	-7	-7	-3.7	-7	-7	-3.7	
By Diameter;																			
	Surface			Top of the Tunnel			Bottom of the Tunnel			Top of the Tunnel Wall			Bottom of the Tunnel Wall						
	4 m	5 m	6 m	4 m	5 m	6 m	4 m	5 m	6 m	4 m	5 m	6 m	4 m	5 m	6 m	4 m	5 m	6 m	
Peak Horizontal Disp. (cm)	+4.5, -5.5	+5.5, -4.5	+5.8, -4.2	+9.7, -3	+9, -2	+7.4, -1.5	+19, -7	+20, -7	+20, -6	+10, -3	+9.5, -2	+7, -1.5	+19, -6	+20, -6	+21, -5	+19, -6	+20, -6	+21, -5	
Peak Vertical Disp. (cm)	-15	-12	-14	-13.5	-13	-15	-7.7	-6.5	-5.5	-15	-14	-16	+2, -6.8	+1.5, -6	+1.3, -5	+2, -6.8	+1.5, -6	+1.3, -5	
Ultimate Horizontal Disp. (cm)	-2	+3	+2.5	+1	+5	+7	-1	+6	+19	+1	+5	+7	-1	+6	+20	-1	+6	+20	
Ultimate Vertical Disp. (cm)	-15	-12	-14	-13.5	-13	-15	-7.7	-6.5	-5.5	-15	-14	-16	-6.8	-6.8	-5	-6.8	-6.8	-5	

One of the most important phenomena occurring in the soil as a result of dynamic effects is liquefaction. The increase in pore water pressures as a result of liquefaction will cause a decrease in the shear strength and stiffness of the soil, and it will also cause stability losses in the structures in liquefied soils. The presence of liquefiable layers will significantly affect the deformation of the underground structure. As a result, the formation of the ground is of great importance when designing tunnels to be built in regions with high seismic activity.

This study focused on the modeling of a three-layered soil system that incorporates a liquefiable layer. The soil formation considered in the analysis was based on the characteristics of the Adapazarı region, which is known to experience significant occurrences of liquefaction. The numerical models of varying depths, diameters, and thicknesses were developed using FLAC 2D, a software capable of simulating changes in pore water pressure. This allowed for the examination of pore water pressure variations within the models. The objective of this study is to investigate the differences in soil deformation under conditions of liquefaction and non-liquefaction. The research aims to analyze and compare the extent of deformations observed in the soil in both scenarios. The constitutive models play a crucial role in numerical modeling, as demonstrated in this study where the Mohr-liquefaction can be modeled, are different from the models obtained from Mohr-Coulomb, reveals the importance of defining the soil behavior in numerical analysis. Similar findings have observed in Beaty and Perlea (2011); upon evaluating the vertical Mohr-Coulomb model exhibited lower displacements compared to the Finn-Byrne model.

The deformations occurring at the points analyzed beneath the tunnel can be interpreted with greater accuracy due to the presence of a liquefiable intermediate layer within the soil formation. The instability experienced in the intermediate layer also had an impact on the upper layers. The soil layers within the depth range of 0 m-20 m exhibit lower SPT values compared to the layers at a depth of 20 m-30 m. As a result, it is anticipated that fewer deformations will be observed in tunnels positioned closer to the bottom layer, considering the trend of decreasing SPT values with depth.

In the models without liquefaction, the influence of thickness on deformations was studied. Interestingly, other studies have suggested that the thickness effect is

not evident in deformations observed in models experiencing liquefaction (Azadi and Hosseini 2010, Unutmaz 2014). Similar to the liquefiable models, the non-liquefiable models did not exhibit a significant impact of thickness on deformations.

Based on this study, it has observed that selection of routes attentively for tunnel placement can minimize their susceptibility to dynamic effects. Additionally, the choice of appropriate soil behavior models for numerical analysis is crucial in accurately modeling liquefaction resulting from dynamic effects.

Declaration of Ethical Standards

The authors of this article declare that the materials and methods used in this study do not require ethical committee permission and/or legal-special permission.

Credit Authorship Contribution Statement

İsa VURAL: Conceptualization, supervision, methodology, review

Dua KAYATÜRK: Visualization, writing – review and editing, formal analysis

Ayşe SAÇAR: Conceptualization, software, formal analysis

Declaration of Competing Interest

The authors declare that they have no known competing financial interests or personal relationships that could have appeared to influence the work reported in this paper.

5. References

- Allen C.R. 1982. Comparison between the North Anatolian fault of Turkey and the San Andreas fault of California. In: Isikara A.M. and Vogel A. (eds), *Multidisciplinary Approach to Earthquake prediction. Proceedings of the International Symposium on Earthquake Prediction in the North Anatolian Fault Zone held in Istanbul, March 31–April 5, 1980. Vol. II.* Vieweg, Braunschweig, 67–75.
- ASTM International, 2006. *Standard Practice for Classification of Soils for Engineering Purposes (Unified Soil Classification System).* ASTM D2487-06. ASTM International, WestConshohocken, PA.
- Azadi M., Hosseini S. M. M. M., 2010. Analyses of the Effect of Seismic Behavior of Shallow Tunnels in Liquefiable Grounds, *Tunnelling and Underground Space Technology*, **25**, 543-552.
- Beaty M. H. and Perlea V. G., 2011. Several Observations on Advanced Analyses with Liquefiable Materials.

- 31th Annual USSD Conference, U. S. Society on Dams, San Diego, California. 1369-1397.
- Byrne, P. M. 1991. A Cyclic Shear-Volume Coupling and Pore-Pressure Model for Sand, Second International Conference on Recent Advances in Geotechnical Earthquake Engineering and Soil Dynamics, St. Louis, Missouri, March. Paper No. 1.24, 47-55.
- Cetin, K. O., Armen Der Kiureghian, and Raymond B. Seed. 2002. Probabilistic Models for the Initiation of Seismic Soil Liquefaction. *Structural Safety* **24** (1): 67–82. [https://doi.org/10.1016/S0167-4730\(02\)00036-X](https://doi.org/10.1016/S0167-4730(02)00036-X).
- FLAC 2D, User's Manual-Fast Lagrangian Analysis of Continua, Itasca Consulting Group, Minnesota.
- Hashash Y.M.A., Hook J.J., Schmidt B., Yao J.I., 2001. Seismic Design and Analysis of Underground Structures, *Tunnelling and Underground Space Technology*, **16**, 247-293.
- Huang, Y., Yu, M. 2013. Review of soil liquefaction characteristics during major earthquakes of the twenty-first century. *Nat Hazards* **65**, 2375–2384 (2013). <https://doi.org/10.1007/s11069-012-0433-9>
- Iida H., Hiroto T., Yoshida N., Iwafuji, 1996. Damage to Daikai subway Soils and Foundations, Special Issue on Geotechnical Aspects of Hyogoken-Naambu Earthquake, *Japanese Geotechnical Society*, **36**, 280-300..
- Kutanis M., Arman H., Firat S., Gündüz Z., 2002. 17 Ağustos 1999 Marmara Depremi ve Adapazarı Bölgesinde Gözlemlenen Deprem Hasarları, IV. Mühendislik ve Mimarlık Sempozyumu, Balıkesir, 459-460..
- Mahmoud, A. O., Hussien, M. N., Karray, M., Chekired, M., Bessette, C., & Jinga, L., 2020. Mitigation of liquefaction-induced uplift of underground structures. *Computers and Geotechnics*, **125**, 103663.
- Ueng T.S., Lin M.L., Chen M.H., 2001. Some geotechnical aspects of 1999 Chi-Chi, Taiwan earthquake, Proceeding of the Fourth International Conference on Recent Advances in Geotechnical Earthquake Engineering and Soil Dynamics, SPL-10, 1-5.
- Unutmaz B., 2014. 3D Liquefaction Assessment of Soils Surrounding Circular Tunnels, *Tunnelling and Underground Space Technology*, **40**, 85-94.
- Vural İ., 2012., Alüvyal ve Sıvılaşılabilen Zeminlerde Altyapıların Deprem Risk Analizi: Adapazarı Örneği, (Doktora tezi), Sakarya Üniversitesi, Fen Bilimleri Enstitüsü, 160.
- Wang, T. T., Kwok, O. L. A., & Jeng, F. S., 2021. Seismic response of tunnels revealed in two decades following the 1999 Chi-Chi earthquake (Mw 7.6) in Taiwan: A review. *Engineering Geology*, **287**, 106090.
- Wang, Z. Z., and Z. Zhang. 2013. Seismic Damage Classification and Risk Assessment of Mountain Tunnels with a Validation for the 2008 Wenchuan Earthquake. *Soil Dynamics and Earthquake Engineering* 45: 45–55. <https://doi.org/10.1016/J.SOILDYN.2012.11.002>.
- Zhuang, H., Hu, Z., Wang, X., & Chen, G., 2015. Seismic responses of a large underground structure in liquefied soils by FEM numerical modelling. *Bulletin of Earthquake Engineering*, **13**, 3645-3668.